Chance-Constrained Optimization for Contact-rich Systems using Mixed Integer Programming

Shirai, Yuki; Jha, Devesh K.; Raghunathan, Arvind; Romeres, Diego

Abstract

Chance-Constrained Optimization for Contact-rich Systems using Mixed Integer Programming Yuki Shirai1, Devesh Jha2, Arvind U Raghunathan2, and Diego Romeres2 1Department of Mechanical and Aerospace Engineering, University of California Los Angeles, CA 90095, USA. email: yukishirai4869@g.ucla.edu 2Mitsubishi Electric Research Laboratories, 201 Broadway, Cambridge, MA 02139, USA. email: jha,raghunathan,romeres@merl.com Abstract Stochastic and robust optimization of uncertain contact-rich systems is relatively unexplored. This paper presents a chance-constrained formulation for robust trajec- tory optimization during manipulation. In particular, we present chance-constrained optimiza- tion of Stochastic Discrete-time Linear Complementarity Systems (SDLCS). The optimiza- tion problem is formulated as a Mixed-Integer Quadratic Program with Chance Constraints (MIQPCC). In our formulation, we explicitly consider joint chance constraints for comple- mentarity variables and states to capture the stochastic evolu- tion of dynamics. Additionally, we demonstrate the use of our proposed approach for designing a Stochastic Model Predic- tive Controller (SMPC) with complementarity constraints for a planar pushing system. We evaluate the robustness of our optimized trajectories in simulation on several systems. The proposed approach outperforms some recent approaches for robust trajectory optimization for SDLCS.

Chance-Constrained Optimization for Contact-rich Systems using Mixed Integer Programming

Yuki Shirai[1], Devesh Jha[2], Arvind U Raghunathan[2], and Diego Romeres[2]

[1]Department of Mechanical and Aerospace Engineering, University of California

Los Angeles, CA 90095, USA. email: `yukishirai4869@g.ucla.edu`

[2]Mitsubishi Electric Research Laboratories, 201 Broadway, Cambridge, MA 02139, USA.

email: {`jha,raghunathan,romeres`}@merl.com

Abstract

Stochastic and robust optimization of uncertain contact-rich systems is relatively unexplored. This paper presents a chance-constrained formulation for robust trajectory optimization during manipulation. In particular, we present chance-constrained optimization of Stochastic Discrete-time Linear Complementarity Systems (SDLCS). The optimization problem is formulated as a Mixed-Integer Quadratic Program with Chance Constraints (MIQPCC). In our formulation, we explicitly consider joint chance constraints for complementarity variables and states to capture the stochastic evolution of dynamics. Additionally, we demonstrate the use of our proposed approach for designing a Stochastic Model Predictive Controller (SMPC) with complementarity constraints for a planar pushing system. We evaluate the robustness of our optimized trajectories in simulation on several systems. The proposed approach outperforms some recent approaches for robust trajectory optimization for SDLCS.

Keywords— discrete-time linear complementarity system, stochastic system, chance-constrained optimization, model predictive control

1 Introduction

Contacts are central to most manipulation problems. Consequently, contact modeling has been an active area of research in robotics since the last several decades [1, 2, 3, 4, 5, 6]. One of the most popular approaches to model contact dynamics is using Linear Complementarity Problem (LCP). The distinguishing feature of a complementarity problem is the set of complementarity conditions. Each of these conditions requires that the product of two or more non-negative quantities (either a decision variable, or a function of decision variables) should be zero [7]. Linear Complementarity Systems have been widely used to succintly represent hybrid dynamical systems [8]. LCP models are widely used for modeling contact dynamics since they allow a compact representation of hybrid dynamics compared to mode enumeration. They have been also used in several physics simulation engines such as Bullet, ODE, etc. Consequently, linear complementarity systems have been extensively explored in robotics research in various domains like manipulation and locomotion.
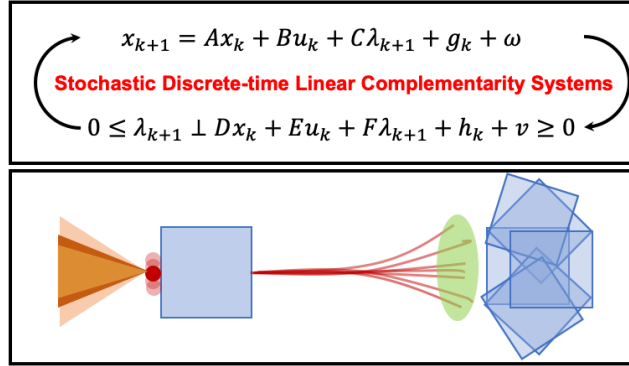
Figure 1: This paper presents chance-constrained optimization for SDLCS. The figure shows the case of stochastic planar pushing with uncertain dynamics. Note that w and v are additive uncertainty terms. We show a Mixed Integer Program (MIP)-based stochastic MPC formulation for control of stochastic planar pushing system.

For example, contact-implicit trajectory optimization (CITO) models contacts as complementarity constraint between contact forces and relative accelerations, and the optimization is formulated as a mathematical program with complementarity constraints (MPCC) [9]. Such techniques have been widely used to solve complex manipulation [10, 11, 12] and locomotion problems [13]. Similarly, Lyapunov stability of linear systems with complementarity systems has also been studied [14, 15, 16]. However, almost all of these works assume deterministic contact models for planning. In reality, contact-rich systems could suffer from several uncertainties which lead to stochastic dynamics and thus, it is important to consider uncertainty during planning. Modeling uncertainty in LCP-based contact models leads to a Stochastic Discrete-time Linear Complementarity System (SDLCS).

Figure 1 shows an example of a stochastic planar pushing system which naturally leads to stochastic evolution of system states due to stochastic frictional interaction during pushing. However, the complementarity constraints in SDLCS pose unique challenges for formulation of robust or stochastic optimization of SDLCS. This is mostly because of the non-differentiability of the complementarity constraints which makes uncertainty propagation challenging. In some recent works that consider stochastic complementarity constraints, an expected residual minimization (ERM)-based [17] penalty is used to solve the robust optimization problem [18]. A major shortcoming of such an approach is that it fails to capture the stochastic evolution of system dynamics due to the stochastic complementarity constraint. Similarly, in [19], the authors augment the formulation in [18] with chance constraints. However, this formulation has certain fundamental shortcomings which prevent constraint satisfaction guarantees. One should notice that uncertainty naturally leads to stochastic evolution of system states in SDLCS. A robust optimization formulation for SDLCS should consider the uncertainty in state evolution. Motivated by these problems and weaknesses, we present a formulation that circumvents these shortcomings by using a mixed integer formulation. Using a relaxation of the complementarity constraints, we formulate the chance-constrained optimization for SDLCS as a Mixed Integer Quadratic Program with Chance Constraints (MIQPCC).

Since worst-case robust optimization is quite conservative and does not explicitly discuss stochastic evolution of states [20], this work considers probabilistic optimization with stochastic evolution of states. We illustrate some challenges in performing principled stochastic optimization for SDLCS. We introduce some simplifying assumptions which are important in order to formulate a tractable optimization problem. In particular, we consider the case where the coefficient matrices multiplying the complementarity variables are stochastic while assuming that the complementarity variables are deterministic. This corresponds to the case when one might have uncertainty arising from errors

2

in parameter identification leading to a SDLCS. An alternative to this, and more accurate formulation, is to allow the complementarity variables to also be stochastic. However, such treatment is out of the scope of the current work. Our treatment of SDLCS leads to stochastic evolution of system states, while we treat the complementarity variables as deterministic. The assumption of determinacy in complementarity variables is similar to several previous works [17], [18], [19], [21]. Robustness to uncertainty is provided by enforcing probabilistic satisfaction of state constraints. Under certain simplifications, we show that the chance-constrained problem can be reformulated as a MIQPCC.

Contributions. This paper has the following contributions:

1. We present a novel formulation for chance-constrained optimization of SDLCS.

2. The proposed optimization is used in a stochastic MPC method for control of stochastic nonlinear complementarity systems.

3. We compare our proposed approach with several previously proposed techniques and demonstrate that our method outperforms the recent techniques in [18, 19].

An initial version of this paper appeared in a conference [22]. The conference version of the paper presented the MIQP formulation for robust optimization. The proposed method was demonstrated on two SDLCS. However, compared to the previously presented work, this work has the following additional contributions:

1. We have included another system (a dual manipulation system) to demonstrate robustness to uncertain friction parameters. We present insights regarding some of the key assumptions made in the proposed formulation.

2. We present a formulation for performing stochastic MPC for stochastic complementarity systems using the proposed formulation. The proposed MPC formulation is verified using a stochastic planar pushing system.

This paper is organized as follows. In Section 2, we present some literature which is close to the proposed work. A problem statement with some required background in Section 3. The robust trajectory formulation is presented in Section 4. Section 5 shows numerical simulations for validation of the proposed formulation. Section 6 presents results for the stochastic MPC for planar pushing problem. Finally, the paper is concluded with some possible future directions in Section 7.

2 Related Work

Our work is closely related to trajectory optimization techniques for contact-rich systems. Contact-Implicit Trajectory Optimization (CITO) techniques are very popular for performing TO for contact-rich systems, and several methods have been proposed for manipulation as well as legged locomotion [9, 23]. More recently, these methods have been extended to formulate fast MPC for contact-rich systems [24]. All the above techniques assume perfect model knowledge and do not consider uncertainty. Planning with uncertain contact-rich systems is relatively unexplored. This is primarily because it is not clear how to propagate uncertainty through the complementarity system for planning. Very recently, there has been some work done in this area and we describe them next.

Recent work on robust trajectory optimization in contact-rich systems can be found in [18, 19, 25]. In [18], the authors have utilized the formulation of expected residual minimization

(ERM) [17] for robust TO. ERM, first introduced in [17] for Stochastic Linear Complementarity Problem (SLCP), aims at minimizing the expected error in satisfying the SLCP. In [18], authors use ERM as an additional penalty term in their TO problem. However, such a formulation does not consider the stochastic state evolution of the system during optimization. A chance-constrained formulation for the stochastic nonlinear complementarity system is presented in [19]. This method augments the ERM-augmented objective in [18] with additional chance constraints on satisfying the complementarity constraints. The formulation ignores the stochastic evolution of system state during optimization, and thus borrows the limitations of [18]. Furthermore, this formulation is incapable of enforcing a constraint violation probability smaller than 0.5 for any degree of uncertainty. Consequently, this method is very fragile for trajectories with horizon lengths longer than one ($N > 1$), as the chance of violating the constraints for such trajectories is $0.5N \geq 1$ [26]. Our formulation addresses these weaknesses under certain simplifying assumptions for SDLCS. More recently, there has been another work which makes use of particles to perform uncertainty propagation in SDLCS [27]. However, the resulting optimization could become computationally challenging. In contrast, this method formulates a computationally efficient method at the cost of some simplifying assumptions.

Another line of work which is relevant to our proposed work is related to Chance-Constrained Optimization (CCO). This has been extensively studied in robotics as well as in the optimization literature [28, 29, 30]. In [28], authors have proposed stochastic optimization formulation for open-loop collision avoidance problems using chance constraints under Gaussian noise. The authors in [30] use statistical moments of the distribution to handle non-Gaussian chance constraints. An important point to note here is that in all CC formulation for dynamic optimization, one needs to consider the Cumulative Density Function (CDF) function for the joint probability distribution of all variables. However, such distribution is extremely challenging to compute. Thus, in general, the joint chance constraint is decomposed into individual chance constraints using Boole's inequality (see [28, 30]), which results in very conservative approximation of the individual constraints. We also utilize Boole's inequality to convert the original computationally intractable joint chance constraints into conservative but tractable independent chance constraints.

3 Problem Preliminary

For completeness of the paper, we first provide a brief introduction to linear complementarity problems and their stochastic form. Then the problem formulation for robust trajectory optimization of stochastic linear complementarity systems is provided. We also point out several key differences of our approach w.r.t. previous attempts for robust trajectory optimization of stochastic complementarity system.

3.1 Discrete-time Linear Complementarity System (DLCS)

A DLCS is a discrete-time linear dynamical system with complementarity constraints [16] represented by:

$$x_{k+1} = Ax_k + Bu_k + C\lambda_{k+1} + g_k \tag{1a}$$

$$0 \leq \lambda_{k+1} \perp Dx_k + Eu_k + F\lambda_{k+1} + h_k \geq 0 \tag{1b}$$

where k is the time-step index, $x_k \in \mathbb{R}^{n_x}$ is the state, $u_k \in \mathbb{R}^{n_u}$ is the control input, and $\lambda_k \in \mathbb{R}^{n_c}$ is the algebraic variable (e.g., contact forces). The matrices, A, B, C, D, E, F and vectors g_k, h_k are of compatible dimensions. The i-th element of vector p_k (p_k can be x_k, u_k, λ_k) is represented as

$p_{k,i}$. The i-th diagonal element of matrix P_k is represented as $P_{k,ii}$. The notation $0 \leq a \perp b \geq 0$ denotes the complementarity constraints $a \geq 0, b \geq 0, ab = 0$. The variables a and b are known as complementarity variables. These variables could be decision variables or functions of decision variables.

Given a pair of state and control values x_k, u_k, a unique solution λ_{k+1} to (1b) exists if F is P-matrix [31]. The matrix F is said to be a P-matrix if every principal minor of F is positive. If F does not satisfy the P-matrix property, it is possible that λ_{k+1} satisfying (1b) is non-unique or non-existent.

3.2 Contact-Implicit Trajectory Optimization

Trajectory optimization for the DLCS (1) can be formulated as:

$$\min_{x,u,\lambda} \sum_{k=0}^{N-1} J(x_k, u_k, \lambda_k) \tag{2a}$$

$$\text{s.t. } x_{k+1} = Ax_k + Bu_k + C\lambda_{k+1} + g_k, \tag{2b}$$

$$0 \leq \lambda_{k+1} \perp Dx_k + Eu_k + F\lambda_{k+1} + h_k \geq 0, \tag{2c}$$

$$x_0 = x_s, x_N = x_g, x_k \in \mathcal{X}, u_k \in \mathcal{U}, \lambda_k \leq \lambda_u \tag{2d}$$

where x_s, x_g represent the initial and the terminal values, respectively, $\mathcal{X} \subseteq \mathbb{R}^{n_x}$ and $\mathcal{U} \subseteq \mathbb{R}^{n_u}$ are convex polytopes consisting of a finite number of linear inequality constraints, λ_u is the upper bound of λ_k, and N is the time horizon. This approach is widely known as contact-implicit trajectory optimization in locmotion and manipulation literature [13, 9, 32].

While (2) is widely used in various robotic applications (see [11, 13]), it can be fragile under uncertainty, which is often the case in model-based manipulation. It is desirable to consider a robust version of the optimization problem in (2). However, the non-differentiability of complementarity constraints pose unique challenges for uncertainty propagation. We present a novel, stochastic version of (2) so that the resulting trajectory would be robust under uncertainty.

3.3 Stochastic Discrete-time Linear Complementarity Systems (SDLCS)

We consider the following SDLCS:

$$x_{k+1} = Ax_k + Bu_k + C\lambda_{k+1} + g_k + w_k \tag{3a}$$

$$0 \leq \lambda_{k+1} \perp y_{k+1} \geq 0 \tag{3b}$$

where $y_{k+1} = Dx_k + Eu_k + F\lambda_{k+1} + h_k + v_k$, and $w_k \in \mathbb{R}^{n_x}, v_k \in \mathbb{R}^{n_c}$ are known additive uncertainties. The variables y_{k+1} and λ_{k+1} are the complementarity variables. One should notice that SDLCS would lead to stochastic evolution of states as well as the complementarity variables. In fact, in a recent publication [27], authors have shown the stochastic evolution of SDLCS. However, the resulting distribution of the complementarity variables is quite complex, which makes uncertainty propagation for SDLCS quite challenging. Thus, we consider the case where the coefficient matrix C in (3a) and F in (3b) are stochastic while the complementarity variables are deterministic. This is used as an alternative approach to model the stochastic effect due to complementarity constraints while admitting a tractable computational approach. Our treatment of SDLCS leads to stochastic evolution of system states x_k, while we treat λ_{k+1} as deterministic. While this assumption is limiting, we show that we can compute robust trajectories for the underlying system.

The authors in [18] use ERM to solve robust TO of SDLCS with the following cost function:

$$\sum_{k=0}^{N-1} \left(J\left(x_k, u_k, \lambda_{k+1}\right) + \beta \mathbb{E}\left[\|\psi\left(\lambda_{k+1}, y_{k+1}\right)\|^2\right] \right) \tag{4}$$

where ψ is a Nonlinear Complementarity Problem (NCP) function and β is a weighting scalar. The NCP function $\psi(\lambda_{k+1}, y_{k+1})$ has the property that $\psi(\lambda_{k+1}, y_{k+1}) = 0$ if and only if the complementarity constraints (3b) hold. An example such a function is $\min(\lambda_{k+1}, y_{k+1})$, where the minimum is applied componentwise. We compare the robustness of our formulation with (4) in Section 5.

4 Robust Trajectory Optimization for SDLCS

In this section, we present our formulation for robust trajectory optimization of SDLCS. We consider the following optimization problem:

$$\min_{x,u,\lambda} \mathbb{E}\left[\sum_{k=0}^{N-1} J(x_k, u_k, \lambda_k)\right] \tag{5a}$$

$$\text{s.t. } x_{k+1} = Ax_k + Bu_k + C\lambda_{k+1} + g_k + w_k, \tag{5b}$$

$$\Pr\left(0 \leq \lambda_{k+1} \perp y_{k+1} \geq 0, x_k \in \mathcal{X}, \forall k\right) \geq 1 - \Delta, \tag{5c}$$

$$x_0 \sim \mathcal{N}\left(x_s, \Sigma_s\right), u_k \in \mathcal{U}, \lambda_k \leq \lambda_u \tag{5d}$$

where $\Pr(\cdot)$ denotes the probability associated with an event and $\Delta \in (0, 0.5]$ is the user-defined maximum probability of violating the constraints. (5c) is the joint chance constraint for the state to lie in the desired set as well as the complementarity constraints at every instant of time. The quantities x_s, Σ_s are the mean and covariance matrix of the state at $k = 0$ respectively . $\mathcal{X}$ and $\mathcal{U}$ are convex polytopes, consisting of a finite number of linear inequality constraints. We make the following simplifying assumptions:

1. The noise terms w_k, v_k follow a Gaussian distribution.

2. The complementarity variable λ_{k+1} is deterministic.

3. Each element of vectors $C\lambda_{k+1}$ and $F\lambda_{k+1}$ are independent Gaussian variables.

Problem (5) might be intractable with this formulation of the constraints (5c). Therefore, in Section 4.1, we propose how to convert (5c) in order to obtain a tractable optimization problem. In Section 4.2 we explain the rationale for the above assumptions as a simplification in order to solve (5) .

We explain the reasoning behind our formulation presented in (5). Since the underlying SDLCS is uncertain, we consider a chance-constrained formulation for optimization to capture stochastic evolution of states where we impose multiple constraints simultaneously. This is represented as joint chance constraints for the complementarity constraints as well as the states, which is succintly written in Equation (5c). Note that we represent the chance constraints on all the variables jointly (as is common in stochastic optimization for dynamic systems) using the cumulative distribution function (cdf) for the state as well as complementarity variables. In the remainder of this section, we will show how the joint constraints can be decomposed into individual chance constraints using Boole's inequality. It is also important to note that unlike the formulation in (5), the method in [18, 19, 33] fails to capture the stochastic evolution of states in their formulation.

4.1 Joint Linear Chance Constraints

We consider joint chance constraint such that multiple constraints are satisfied simultaneously with a pre-specified probability. More specifically, we consider the joint chance constraints (5c) so that the complementarity constraints and state bound constraints over the whole time horizon of the optimized trajectory are satisfied with probability $(1-\Delta)$. We succintly denote the complementarity relationship in (3b) as $(\lambda_{k+1,i}, y_{k+1,i}) \in \mathcal{S}$ for $i = 1, \ldots, n_c$, i.e. $(\lambda_{k+1,i}, y_{k+1,i})$ satisfies (3b) if and only if $(\lambda_{k+1,i}, y_{k+1,i}) \in \mathcal{S}$. Hence, we can rewrite the joint chance constraints in the optimization problem (5) as:

$$\Pr\left(0 \le \lambda_{k+1} \perp y_{k+1} \ge 0, x_k \in \mathcal{X}, \forall k\right) \ge 1 - \Delta \iff$$

$$\Pr\left(\bigwedge_{k=0}^{N}\left(\bigwedge_{i=1}^{n_c}(\lambda_{k+1,i}, y_{k+1,i}) \in \mathcal{S}\right) \bigwedge \left(\bigwedge_{l=1}^{L} a_l^\top x_k \le b_l\right)\right) \tag{6}$$

$$\ge 1 - \Delta$$

where $\bigwedge$ is the logical AND operator. The parameter L represents the number of inequalities modeling $\mathcal{X}$ and $a_l \in \mathbb{R}^{n_x}$ is the coefficient vector and b_l represents the right-hand side of the inequality.

Obtaining a cumulative density function (cdf) of (6) is challenging because the joint probability of states and complementarity variables is considered. A popular approach to decompose joint chance constraints is the application of Boole's inequality [26] which converts the original computationally intractable joint chance constraints into conservative but tractable independent chance constraints. Hence, similar to previous works, we use Boole's inequality [26] to get the conservative approximation of (6) as follows:

$$\Pr\left(\bigwedge_{k=0}^{N}\left(\bigwedge_{i=1}^{n_c}(\lambda_{k+1,i}, y_{k+1,i}) \in \mathcal{S}\right)\right) \ge 1 - \Delta_1,$$

$$\Pr\left(\bigwedge_{k=0}^{N}\left(\bigwedge_{l=1}^{L} a_l^\top x_k \le b_l\right)\right) \ge 1 - \Delta_2, \Delta_1 = \Delta_2 = \frac{\Delta}{2} \tag{7}$$

Using Boole's inequality again, we can further obtain the conservative chance constraints given by:

$$\Pr\left((\lambda_{k+1,i}, y_{k+1,i}) \in \mathcal{S}\right) \ge 1 - \frac{\Delta_1}{Nn_c}, \tag{8a}$$

$$\Pr\left(a_l^\top x_k \le b_l\right) \ge 1 - \frac{\Delta_2}{NL}, \tag{8b}$$

We discuss how to handle (8a) in Section 4.2. We formulate (8b) as its equivalent deterministic form (see [29, 34, 35]):

$$\Pr\left(a_l^\top x_k \le b_l\right) \ge 1 - \frac{\Delta_2}{NL} \iff \tag{9a}$$

$$a_l^\top \bar{x}_k \le b_l - \sqrt{a_l^\top \Sigma_{x_k} a_l} \Phi^{-1}(1 - \frac{\Delta_2}{NL}) \tag{9b}$$

where $\bar{x}_k, \Sigma_{x_k}$ are the mean and covariance matrix of x_k, respectively. Φ^{-1} is an inverse of the cdf of the standard normal distribution.
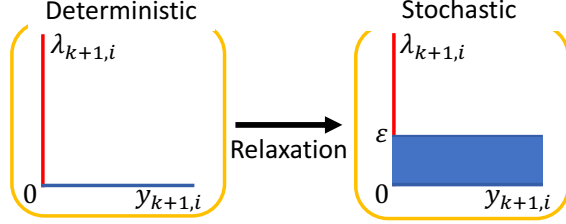
Figure 2: Deterministic and stochastic complementarity constraints. We have the complementarity constraints $0 \leq \lambda_{k+1,i} \perp y_{k+1,i} \geq 0$ where $y_{k+1,i}$ has uncertainty and accepts the violation of ϵ.

4.2 Chance Complementarity Constraints (CCC) for SDLCS

We explain the rationale behind some of the assumptions specified in Section 4. One of the key assumptions is that the complementarity variable λ_{k+1} is deterministic. A more general formulation would allow the complementarity variable λ_{k+1} to be stochastic. Indeed, in our previous work [27], we have shown that the complementarity variable λ_{k+1} is in fact stochastic. One should notice, however, that the complementarity constraints naturally leads to truncated distribution of the complementarity variables (as $\lambda_{k+1} \geq 0$). This makes uncertainty propagation for complementarity variables challenging. This could potentially make the stochastic optimization problem computationally challenging (see [27]). Thus, in this work, we make the assumption that λ_{k+1} is deterministic, which improves the computational requirements for the resulting optimization problem. Furthermore, we believe that allowing C and F to be stochastic can model a similar effect to having λ_{k+1} stochastic in the SDLCS. Finally, note that in cases where the distribution of λ_{k+1} is known, our proposed formulation can be easily extended to incorporate stochasticity in λ_{k+1}. However, for brevity, we skip these details. Assuming the uncertainty to be Gaussian is motivated by our interest in leveraging the equivalent reformulation of the chance constraints to deterministic inequalities.

While [19] proposed a promising CCC, their formulation possesses empty solutions when $\Delta \leq 0.5$ (see [19]). The formulation in [19] can result in a very fragile trajectory since the total violation probability over N steps would be always more than 1 if $N \geq 1$ (using Boole's inequality). Since the optimization is formulated as a Non-Linear Program (NLP), all the CCC are imposed simultaneously. Consequently, the resulting formulation struggles to find feasible solutions.

In our formulation, the stochastic complementarity constraints are decomposed into two modes (see Fig. 2) as follows:

$$\Pr\left((\lambda_{k+1,i}, y_{k+1,i}) \in \mathcal{S}\right) \geq 1 - \theta \tag{10a}$$

$$\Longleftrightarrow \Pr\left(\bigvee \begin{matrix} (\lambda_{k+1,i} \geq 0, y_{k+1,i} = 0) \\ (\lambda_{k+1,i} = 0, y_{k+1,i} \geq 0) \end{matrix}\right) \geq 1 - \theta \tag{10b}$$

$$\Longleftrightarrow \begin{cases} \lambda_{k+1,i} \geq 0, \Pr\left(y_{k+1,i} = 0\right) \geq 1 - \theta \\ \text{or } \lambda_{k+1,i} = 0, \Pr\left(y_{k+1,i} \geq 0\right) \geq 1 - \theta \end{cases} \tag{10c}$$

where $\theta = \frac{\Delta_1}{N n_c}$ and $\bigvee$ denotes the logical OR. Note that now $y_{k+1} \sim \mathcal{N}\left(\bar{y}_{k+1}, \Sigma_{y_{k+1}}\right)$. To obtain lower violation probabilities, we propose an Mixed Integer Programming (MIP) framework. First, we propose the following CCC:

$$z_{k,i,0} = 1, \Longrightarrow \lambda_{k+1,i} \geq 0, \Pr\left(y_{k+1,i} = 0\right) \geq 1 - \theta, \tag{11a}$$

$$z_{k,i,1} = 1, \Longrightarrow \lambda_{k+1,i} = 0, \Pr\left(y_{k+1,i} \geq 0\right) \geq 1 - \theta \tag{11b}$$

8

where $z_{k,i,0}, z_{k,i,1}$ denote the binary variables to represent the two modes which satisfies $z_{k,i,0} + z_{k,i,1} = 1$ for i-th complementarity constraint at instant k.

However, $\Pr(y_{k+1,i} = 0)$ is zero (as the probability measure for singleton sets is zero) so that we cannot directly use (11). To alleviate this issue while avoiding negative values for λ, we propose the following CCC using a relaxation for complementarity constraints (see Fig. 2):

$$z_{k,i,0} = 1, \Longrightarrow \lambda_{k+1,i} \geq 0, \Pr(0 \leq y_{k+1,i} \leq \epsilon) \geq 1 - \theta, \tag{12a}$$

$$z_{k,i,1} = 1, \Longrightarrow \lambda_{k+1,i} = 0, \Pr(y_{k+1,i} \geq \epsilon) \geq 1 - \theta \tag{12b}$$

where $\epsilon > 0$ is the acceptable violation in the complementarity constraints.

We have two-sided linear chance constraints in (12a). We decompose (12a) as two one-sided chance constraints so that we can use the same reformulation as in (9). Note that each one-sided chance constraints, obtained from the two-sided chance constraint, are formulated with a maximum violation probability of $\frac{\theta}{2}$.

Since we have integer constraints, MIP can impose individual constraints for each mode separately. This allows to derive a lower bound for θ as function of ϵ, $\bar{y}_{k+1,i}$, and $\Sigma_{y_{k+1},ii}$, which is presented in Lemma 4.1. On the other hand, the NLP formulation imposes all mode constraints jointly (see [19]). Consequently, the NLP formulation achieves a higher bound for θ. We provide arguments describing the advantage of our approach over the NLP approach in Remark 1.

Lemma 4.1. *Suppose the CCC are formulated as (12) and ϵ, $\bar{y}_{k+1,i}$, and $\Sigma_{y_{k+1},ii}$ are specified. Then (i) (12a) is feasible for all $\theta > 2(1 - \Phi(\frac{\epsilon}{2\Sigma_{y_{k+1},ii}}))$ and (ii) (12b) is feasible for all $\theta > 1 - \Phi\left((\bar{y}_{k+1,i} - \epsilon)/\Sigma_{y_{k+1}ii}\right)$.*

Proof. Consider case (i): From (9b) and (12a), the two-side chance constraints in (12a) are converted to their deterministic forms which are given as: $\Sigma_{y_{k+1},ii}\Phi^{-1}(1 - \theta/2) \leq \bar{y}_{k+1,i} \leq \epsilon - \Sigma_{y_{k+1},ii}\Phi^{-1}(1 - \theta/2)$. To have a nonempty solution, we must have $\epsilon - 2\Sigma_{y_{k+1},ii}\Phi^{-1}(1 - \theta/2) > 0$. Simplifying this equation, we obtain the bound specified in (i). Consider case (ii): From (9b) and (12b), the one-side chance constraints in (12b) are converted as: $\bar{y}_{k+1,i} \geq \epsilon + \Sigma_{y_{k+1},ii}\Phi^{-1}(1 - \theta)$. Simplifying this equation, we obtain the bound specified in (ii). $\square$

Remark 4.1. *From Lemma 4.1, it is easy to show that $\theta < \frac{1}{2}$ if $\frac{\epsilon}{2\Sigma_{y_{k+1},ii}} > \Phi^{-1}(\frac{3}{4})$ for case (i), and if $(\bar{y}_{k+1,i} - \epsilon)/\Sigma_{y_{k+1}ii} > \Phi^{-1}(\frac{1}{2})$ for case (ii). In contrast, the formulation in [19] cannot enforce the chance constraints for any $\theta < 0.5$.*

The evolution of the mean of the states in SDLCS is described by the following equations:

$$\bar{x}_{k+1} = A\bar{x}_k + Bu_k + \overline{C\lambda}_{k+1} + g_k + \bar{w}_k, \tag{13a}$$

$$\Sigma_{x_{k+1}} = A\Sigma_{x_k}A^\top + \Sigma_{C\lambda_{k+1}} + W \tag{13b}$$

where W represents the noise covariance matrix and $\overline{C\lambda}_{k+1}$ represents a mean of $C\lambda_{k+1}$, and $\Sigma_{C\lambda_{k+1}} = \mathbb{E}\left[\left(C\lambda_{k+1} - \overline{C\lambda}_{k+1}\right)\left(C\lambda_{k+1} - \overline{C\lambda}_{k+1}\right)^\top\right]$ is a diagonal matrix because of the independence of random variables.

The mean and variance of y_k in SDLCS is described by the following equations:

$$\bar{y}_k = D\bar{x}_k + Eu_k + \overline{F\lambda}_{k+1} + h_k + \bar{v}_k, \tag{14a}$$

$$\Sigma_{y_k} = D\Sigma_{x_k}D^\top + \Sigma_{F\lambda_{k+1}} + V \tag{14b}$$

where V represents the noise covariance matrix from v_k and $\overline{F\lambda}_{k+1}$ represents a mean of $F\lambda_{k+1}$, and $\Sigma_{F\lambda_{k+1}} = \mathbb{E}\left[\left(F\lambda_{k+1} - \overline{F\lambda}_{k+1}\right)\left(F\lambda_{k+1} - \overline{F\lambda}_{k+1}\right)^\top\right]$ is a diagonal matrix because of the independence of random variables.

4.3 Mixed-Integer Quadratic Programming with Chance Constraints (MIQPCC)

In this section, we present our MIQPCC formulation to solve (5). The proposed CCC could be imposed in either an MIP or an NLP framework. However, our MIP-based method solves disjunctive inequalities while NLP needs to impose all CCC simultaneously, which yields an empty solution for $\Delta \le 0.5$. For this reason we do not consider an NLP framework.

The proposed MIQPCC is formulated as follows:

$$\min_{x,u,\lambda,z} \sum_{k=0}^{N-1} \bar{x}_k^\top Q \bar{x}_k + u_k^\top R u_k \tag{15a}$$

$$\text{s. t. } \bar{x}_{k+1} = A\bar{x}_k + Bu_k + \overline{C\lambda}_{k+1} + g_k + \bar{w}_k, \tag{15b}$$

$$\Sigma_{x_{k+1}} = A\Sigma_{x_k}A^\top + \Sigma_{w,C\lambda_{k+1}} + W, \tag{15c}$$

$$x_0 \sim \mathcal{N}(x_s, \Sigma_s), u_k \in \mathcal{U}, \lambda_k \le \lambda_u, \tag{15d}$$

$$a_l^\top \bar{x}_k \le b_l - \alpha\kappa, \tag{15e}$$

$$z_{k,i,0} + z_{k,i,1} = 1, \tag{15f}$$

$$0 \le \lambda_{k+1,i} \le M z_{k,i,0}, \tag{15g}$$

$$\zeta\psi z_{i,k,0} + (\epsilon + \eta\psi)z_{k,i,1} \le \bar{y}_{k+1,i} \tag{15h}$$

$$\bar{y}_{k+1,i} \le (\epsilon - \zeta\psi)z_{k,i,0} + M z_{k,i,1}, \tag{15i}$$

where $Q = Q^\top \ge 0, R = R^\top > 0$, $\alpha = \Phi^{-1}(1 - \frac{\Delta}{2NL}), \zeta = \Phi^{-1}(1 - \frac{\Delta}{4Nn_c}), \eta = \Phi^{-1}(1 - \frac{\Delta}{2Nn_c}), \kappa = \sqrt{a_l^\top \Sigma_{x_k} a_l}, \psi = \sqrt{\Sigma_{y_{k+1,ii}}}$. $z_{k,i,0}, z_{k,i,1}$ are the binary decision variables for the i-th complementarity constraint at k to represent mode 1, 2, respectively. Using these binary variables, we employ big-M formulation to deal with disjunctive inequalities in our CCC. The parameter M is a valid upper bound for λ_k, y_k.

4.4 Stochastic Model Predictive Control (SMPC) with Complementarity Constraints

Model Predictive Control (MPC) is very popular and well understood for control of smooth dynamical systems. However, it remains mostly unexplored for complementarity systems and stochastic complementarity systems. Using our proposed MIQPCC, we present a stochastic MPC method for uncertain contact systems. More formally, we present a formulation to implement SMPC for stochastic non-linear complementarity system (SNCS) where the dynamics equation is represented as:

$$x_{k+1} = f(x_k, u_k, \lambda_{k+1}) + w_k \tag{16a}$$

$$0 \le \lambda_{k+1} \perp y_{k+1} \ge 0 \tag{16b}$$

where $f(x_k, u_k, \lambda_{k+1})$ is nonlinear dynamics. The goal is to find a control sequence to track a reference state trajectory for the SNCS. We first create the reference trajectory x^*, u^*, λ^*, y^* by solving the optimization with deterministic complementarity constraints (no chance constraints) using Mathematical Program with Complementarity Constraints (MPCC) [9]. Then, we linearize the dynamics along the reference trajectory which is used for uncertainty propagation.

10

The modified MIQPCC for SMPC is given by:

$$\min_{x,u,\lambda,z} x_N^{e\top} Q_N x_N^e + \sum_{k=0}^{N-1} x_k^{e\top} Q x_k^e + u_k^{e\top} R u_k^e \tag{17a}$$

$$\text{s.t.} x_{k+1}^e = A x_k^e + B u_k^e + C\lambda^e_{k+1} + \bar{w}_k, \tag{17b}$$

$$(15c), (15e), (15f), \tag{17c}$$

$$x_0 \sim \mathcal{N}(x_s, \Sigma_s), u_k^e + u_k^* \in \mathcal{U}, \lambda_k^e + \lambda_k^* \leq \lambda_u, \tag{17d}$$

$$0 \leq \lambda_{k+1,i}^e + \lambda_{k+1,i}^* \leq M z_{k,i,0} \tag{17e}$$

$$\zeta\psi z_{i,k,0} + (\epsilon + \eta\psi)z_{k,i,1} \leq y_{k+1,i}^e + y_{k+1,i}^* \tag{17f}$$

$$y_{k+1,i}^e + y_{k+1,i}^* \leq (\epsilon - \zeta\psi)z_{k,i,0} + M z_{k,i,1} \tag{17g}$$

where $x^e = \bar{x} - x^*, u^e = u - u^*, \lambda^e = \lambda - \lambda^*, y^e = \bar{y} - y^*, A = \left.\frac{\partial f(x,u,\lambda)}{\partial x}\right|_{x^*,u^*,\lambda^*}, B = \left.\frac{\partial f(x,u,\lambda)}{\partial u}\right|_{x^*,u^*,\lambda^*}, C = \left.\frac{\partial f(x,u,\lambda)}{\partial \lambda}\right|_{x^*,u^*,\lambda^*}$. It is worth pointing out that this formulation does not fix or penalize the discrete mode sequence. (17e) means that $\lambda_{k+1,i} \geq 0$ if $z_{k,i,0} = 1$ and $\lambda_{k+1,i} = 0$ if $z_{k,i,1} = 1$. Thus, (17e) allows deviation from the reference discrete mode sequence while satisfying complemenatarity constraints. Therefore, the controller may change the mode sequence from the reference. In prior work, Hogan et al. [36] proposed a similar MIQP formulation. However, they penalize deviation from the reference mode sequence which might be infeasible for a number of cases (due to state and control bounds). Additionally, it does not consider stochastic dynamics and complementarity constraints during control.

5 Numerical Simulations

We validate our proposed method using three benchmark DLCS which are shown in Fig. 3. See [15] for more details of these three benchmarks. Through the numerical experiments performed in the paper, we answer the following questions:

1. Can our proposed optimization generate robust open-loop trajectories?

2. Can our proposed formulation satisfy the probabilistic constraints imposed during optimization?

3. How does the proposed method compare against the previous methods for robust optimization in SDLCS?

5.1 Implementation Details

The proposed method is implemented in Python. We use Gurobi [37] to solve the proposed MIQPCC, and PyRoboCOP [9, 38] to solve the MPCC arising from the ERM-based method in [18] and the CCC method in [19]. The examples are implemented on a computer with Intel i7-12800H processor.

We verify the robustness of open-loop trajectories obtained from our proposed optimization using Monte Carlo simulations. To simulate SDLCS with a given control input, we use MINPACK [39] to solve the nonlinear complementarity problem that arises at each time-step in order to simulate the system. The noise term is sampled from the distribution which was used during optimization. We

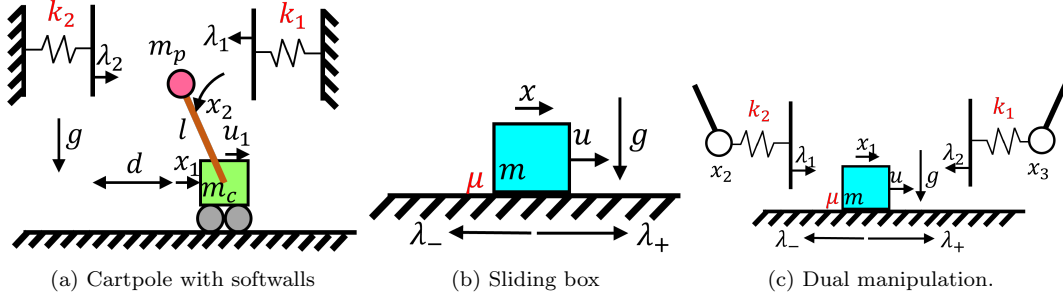(a) Cartpole with softwalls   (b) Sliding box   (c) Dual manipulation.

Figure 3: Problems described in Section 5.

simulate each control trajectory for 1000 times to estimate the probability of constraint violation for the proposed as well as the baseline methods.

For notation simplicity, we present the continuous-time dynamics for all the test systems. We discretize continuous-time dynamics into discrete-time dynamics using the explicit Euler method with sample time $dt = 0.033$. We denote x_0, Σ_0 as the mean and covariance matrix at $k = 0$ for states of systems, respectively.

5.2 Example Details

5.2.1 Cartpole with Softwalls

The continuous-time dynamics with complementarity constraints for the cartpole with softwalls (see Fig. 3a) is as follows:

$$\dot{x}_1 = x_3, \dot{x}_2 = x_4, \dot{x}_3 = g\frac{m_p}{m_c}x_2 + \frac{1}{m_c}u_1, \tag{18a}$$

$$\dot{x}_4 = \frac{g(m_c + m_p)}{lm_c}x_2 + \frac{1}{lm_c}u_1 + \frac{\lambda_1}{lm_p} - \frac{\lambda_2}{lm_p}, \tag{18b}$$

$$0 \leq \lambda_1 \perp lx_2 - x_1 + \frac{1}{k_1}\lambda_1 + d \geq 0, \tag{18c}$$

$$0 \leq \lambda_2 \perp x_1 - lx_2 + \frac{1}{k_2}\lambda_2 + d \geq 0 \tag{18d}$$

where x_1 is the cart position, x_2 is the pole angle, the x_3 and x_4 are their derivatives. u_1 is the control and λ_1, λ_2 are the reaction forces at from the wall 1, 2, respectively. We consider the additive noise w, the zero-mean i.i.d. Gaussian noise which standard deviation is 2×10^{-4}, to $x_{1,k}, x_{2,k}$. $k_1 = 10, k_2 = 10$ are the stiffness of walls 1 and 2, respectively. In this example, we assume that the uncertainty also arises from the $\frac{1}{k_1}, \frac{1}{k_2}$ which standard deviations are 10^{-5}. We denote by $g = 9.81$ is the gravitational acceleration, and by $m_p = 0.1, m_c = 1.0$ denote the mass of the pole, cart, respectively. Further, $l = 0.5$ is the length of the pole and $d = 0.15$ is the distance from the origin of the coordinate to the walls.

The optimization setup is as follows: $N = 20, M = 100, Q = \text{diag}(0,0,0,0), R = 0.01, \epsilon = 0.002, x_0 = [-0.15, 0, 0, 0]^\top, \Sigma_0 = \text{diag}(0,0,0,0)$. We also impose the following chance constraints: $\Pr(x_{1,k} \leq 0.05) \geq 1 - \frac{\Delta}{4N}, \Pr(x_{2,k} \leq 0.15) \geq 1 - \frac{\Delta}{4N}, \forall k = 0, \ldots, N-1, \Pr(-0.02 \leq x_{1,N} \leq 0.02) \geq 1 - \frac{\Delta}{4N}, \Pr(-0.04 \leq x_{2,N} \leq 0.04) \geq 1 - \frac{\Delta}{4N}$.

5.2.2 Sliding Box with Friction

The continuous-time quasi-static dynamics with complementarity constraints for sliding box with Coulomb friction (see Fig. 3b) is as follows:

$$\dot{x}_1 = x_2, \alpha\dot{x}_1 = u + \lambda_+ - \lambda_-, \tag{19a}$$

$$0 \leq \gamma \perp \mu mg - \lambda_+ - \lambda_- \geq 0, \tag{19b}$$

$$0 \leq \lambda_+ \perp \gamma + u + \lambda_+ - \lambda_- \geq 0, \tag{19c}$$

$$0 \leq \lambda_- \perp \gamma - u - \lambda_+ + \lambda_- \geq 0 \tag{19d}$$

where x_1 is the box position and x_2 is the box velocity. u is the control input and λ_+, λ_- are the positive and negative components of the friction force, respectively. γ is the slack variable. $\alpha = 4$ is the damping constant, $m = 1$ is the mass of the box, and $\mu = 0.1$ is the coefficient of friction. We consider additive i.i.d. Gaussian noise w in the dynamics equation as $x_{1,k+1} = x_{1,k} + x_{2,k}dt + w$. The standard deviation of w is 4×10^{-4}. $g = 9.81$ is the gravitational acceleration. We assume that the coefficient of friction, μ, is also uncertain and standard deviation for μ is 10^{-5}.

The optimization setup is as follows: $N = 20, M = 100, Q = \text{diag}(0,0,0,0), R = 0.01, \epsilon = 0.01, x_0 = [1,-1]^\top, \Sigma_0 = \text{diag}(0,0)$. We also impose the following chance constraints: $\Pr(x_{1,k} \geq 0.885) \geq 1 - \frac{\Delta}{2N}, \forall k = 0,\ldots,N-1, \Pr(0.89 \leq x_{1,N} \leq 0.91) \geq 1 - \frac{\Delta}{2N}, \Pr(-0.1 \leq x_{2,N} \leq 0.1) \geq 1 - \frac{\Delta}{2N}$.

5.2.3 Dual Manipulator System

We consider the example where a box is manipulated on a planar surface with Coulomb friction and contact forces from two manipulators (see Fig. 3c). The continuous-time quasi-static dynamics is as follows:

$$\dot{x}_1 = x_2, \alpha\dot{x}_1 = \lambda_1 - \lambda_2 + \lambda_+ - \lambda_-,$$
$$\dot{x}_3 = x_4, \dot{x}_4 = u_1, \dot{x}_5 = x_6, \dot{x}_6 = u_2,$$
$$0 \leq \lambda_1 \perp x_1 - x_3 + \frac{1}{k}\lambda_1 \geq 0,$$
$$0 \leq \lambda_2 \perp x_5 - x_1 + \frac{1}{k}\lambda_2 \geq 0, \tag{20}$$
$$0 \leq \gamma \perp \mu mg - \lambda_+ - \lambda_- \geq 0,$$
$$0 \leq \lambda_+ \perp \gamma + \lambda_1 - \lambda_2 + \lambda_+ - \lambda_- \geq 0,$$
$$0 \leq \lambda_- \perp \gamma - \lambda_1 + \lambda_2 - \lambda_+ + \lambda_- \geq 0$$

x_1, x_3, x_5 are the positions of the box, the left arm, the right arm, respectively and x_2, x_4, x_6 are their derivatives. u_1, u_2 represent the controls of the left and the right arm, respectively. λ_+, λ_- are the positive and negative component of the friction force, respectively. γ is the slack variable. λ_1, λ_2 are the contact forces from the left arm and the right arm, respectively. We set $g = 9.81$, $m = 1$, $k = 100$, $\mu = 0.1$. We discretize the dynamics (20) with $dt = 0.033$. As in the previous systems, we the zero-mean i.i.d. Gaussian noise w with standard deviation 0.0002 to the dynamics, $x_{1,k+1} = x_{1,k} + x_{2,k}dt + w$. The standard deviation of μ and $\frac{1}{k}$ are 0.0001.

The optimization setup in this example is as follows: $N = 20, M = 50, Q = \text{diag}(0,0,0,0,0,0), R = \text{diag}(1,1), \epsilon = 0.0042, x_0 = [0.1,-1.1,0,0,0.1,0]^\top, \Sigma_0 = \text{diag}(0,0,0,0,0,0)$. We impose the following chance constraints: $\Pr(x_{1,k} \geq -0.17) \geq 1 - \frac{\Delta}{2N}, \forall k = 0,\ldots,N-1, \Pr(-0.01 \leq x_{1,N} \leq 0.01) \geq 1 - \frac{\Delta}{2N}$.
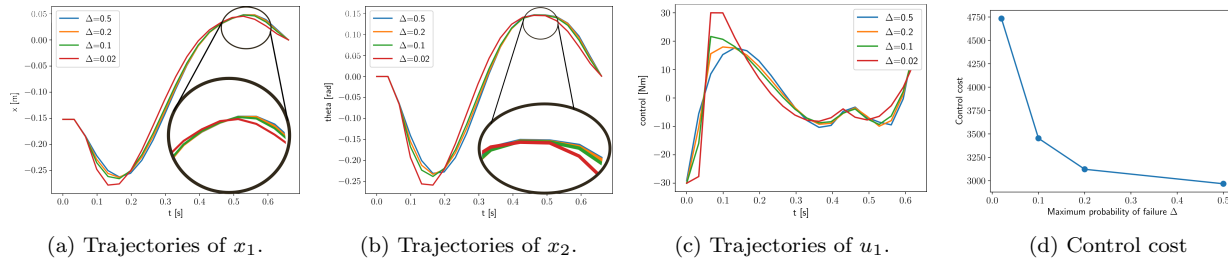
(a) Trajectories of x_1.　　(b) Trajectories of x_2.　　(c) Trajectories of u_1.　　(d) Control cost

Figure 4: Results with different Δ for the cartpole with softwalls system. First, the cart moves in the negative direction to utilize the contact force λ_2 because the control input is bounded. Once the cart obtains enough λ_2, the cart is accelerated in the positive direction. We can observe the effect of our proposed chance constraints in particular around $t \in [0, 0.1]$ and $t \in [0.4, 0.5]$. When $t \in [0, 0.1]$, the mode changes from the "contact on the wall 2" to the "no contact" and the cart tries to be far from wall 2 to satisfy the CCC. When $t \in [0.4, 0.5]$, the trajectories are farther away from $x_1 = 0.05$ and $x_2 = 0.15$ as Δ decreases.

Remark 5.1. *It is noted that the proposed method can be used for robust optimization as long as the dynamics is linear. In the presence of non-linear dynamics, uncertainty propagation becomes more challenging and it can not be modeled by the current framework. The uncertainty in SDLCS can arise from various sources like parametric uncertainty (e.g., coefficient of friction, uncertain stiffness coefficients, etc.). As long as the underlying dynamics can be modeled as a SDLCS, the proposed formulation could be used for robust optimization.*

5.3　Robustness of Open-Loop Trajectories

The optimized control and state trajectories for the three systems using our proposed method are shown in Fig. 4-Fig. 6. Overall, these figures show that the optimal state trajectories move further away from the bound specified in the chance constraints as the violation probability decreases (see the state constraints specified in Section 5.2). For instance, Fig. 4a shows that the computed trajectories move further away from $x = 0.05$ as Δ decreases (note that $\Pr(x_{1,k} \leq 0.05) \geq 1 - \frac{\Delta}{4N}$ is the chance constraint specified for optimization, see Section 5.2). We observe the same behavior for the other systems too in Fig. 5 and Fig. 6. In addition, these figures illustrate that the control costs increase as Δ decreases. This illustrates the trade-off between safety and cost.

Remark 5.2. *At this point, we would like to discuss the magnitude of uncertainty we consider in these problems. Compared to other stochastic optimal control works [28, 29], the uncertainty in these problems is relatively smaller. There are several reasons why we need to have a smaller uncertainty. Note that as we have explained in Section 3, our approach satisfies joint constraints on multiple constraints together. First, our formulation has chance complementarity constraints in addition to chance constraints on states, which are commonly used. Our formulation has more number of chance constraints, and consequently, the lower uncertainty is required because of the conservative approximation of Boole's inequality to resolve joint chance constraints into individual constraints as explained in Section 4.1, and Section 4.2. Second, we need to have a small ϵ to avoid large violation of complementarity constraints, which requires small uncertainty. Finally, we would like to emphasize that allowing larger uncertainties requires either better resolution of joint chance constraints or covariance steering approaches [29, 27], which is out of scope for the current study.*
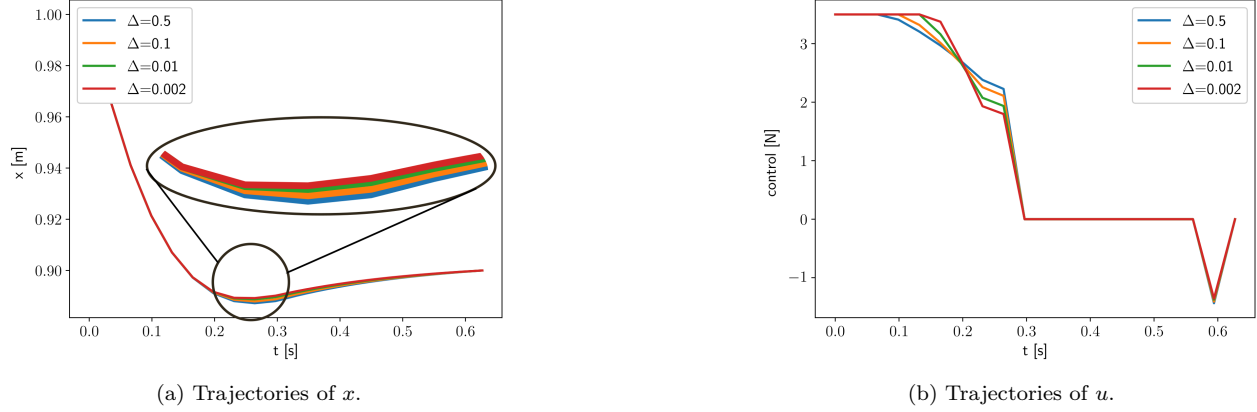
14

(a) Trajectories of x.

(b) Trajectories of u.

Figure 5: Results with different Δ for the sliding box with friction example. First, the box is accelerated in the positive direction. Then, the control decreases with time to regulate the box around the origin by employing friction forces. We can observe the effect of our proposed chance constraints in particular around $t \in [0.2, 0.3]$ where the trajectories are farther away from $x = 0.88$ as Δ decreases.

(a) Trajectories of x_1.

(b) State x_1 around $t \in [0.2, 0.3]$

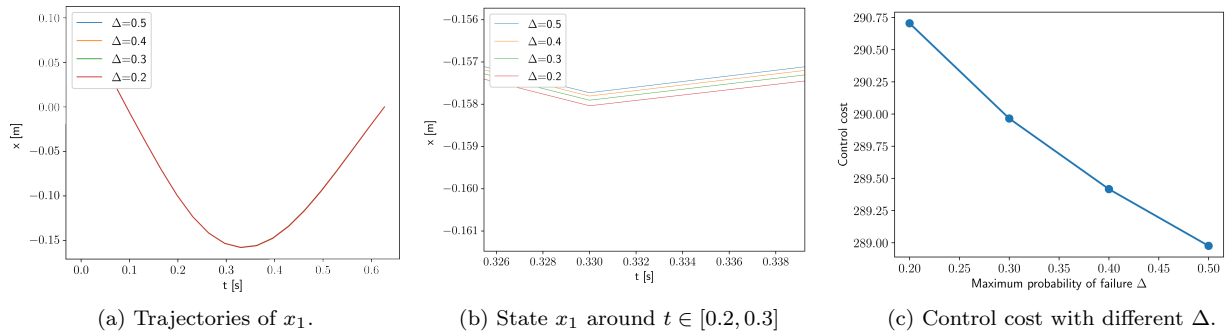(c) Control cost with different Δ.

Figure 6: Results with dual manipulation. First, the box is pushed by the right arm in the negative direction. Next, the left arm regulates the box to the origin. In particular, around $t \in [0.2, 0.3]$ s, the trajectories are farther away from $x_1 = -0.17$ m as Δ decreases.

15

Table 1: Comparison of the constraint violation probability specified in the different optimization problems against the observed constraint probabililty obtained from simulation of the "cartpole with softwalls" over 1000 samples. In the table, Δ represents the constraint violation probability for our approach, β for the ERM-based approach in [18], and the Δ_z is for the CCC method in [19].

	$\Delta = 0.5$	$\Delta = 0.2$	$\Delta = 0.1$	$\Delta = 0.02$
Obtained Δ (Ours)	0.190	0.147	0.085	0.020
	$\beta = 10^3$	$\beta = 10^4$	$\beta = 10^5$	$\Delta_z = 0.5$
Obtained Δ (ERM)	0.75	1.0	1.0	-
Obtained Δ (CCC)	-	-	-	0.91

Table 2: Comparison of the constraint violation probability specified in the different optimization problems against the observed constraint probabililty obtained from simulation of the "a sliding box with friction" over 1000 samples. In the table, Δ represents the constraint violation probability for our approach, β for the ERM-based approach in [18], and the Δ_z is for the CCC method in [19].

	$\Delta = 0.5$	$\Delta = 0.1$	$\Delta = 0.01$	$\Delta = 0.002$
Obtained Δ (Ours)	0.080	0.051	0.027	0.010
	$\beta = 10^3$	$\beta = 10^4$	$\beta = 10^5$	$\Delta_z = 0.5$
Obtained Δ (ERM)	1.0	1.0	1.0	-
Obtained Δ (CCC)	-	-	-	0.91

5.4   Monte Carlo Simulation Results

Table 1-Table 3 present the comparison of constraint violation for the proposed method and the baseline methods proposed in [18] and [19] using Monte Carlo simulation. We compute the empirical constraint violation for all the three problems with different values of Δ. We run the ERM method in [18] with different objective weights β and the CCC [19] with violation probability $\Delta_z = 0.5$ (as discussed in the original paper). The parameter β was chosen so that the magnitude of the ERM cost is of similar order as the other costs in the objective. Since in the original work in [18] and [19], the authors had only considered the terminal constraint violation, we only measure the failure of these methods for violation of the terminal constraint. For the proposed method, we measure the constraint violations which was specified in Section 5.2.

Table 3: Comparison of the constraint violation probability specified in the different optimization problems against the observed constraint probabililty obtained from simulation of the "dual manipulation" over 1000 samples. In the table, Δ represents the constraint violation probability for our approach, β for the ERM-based approach in [18], and the Δ_z is for the CCC method in [19].

	$\Delta = 0.5$	$\Delta = 0.4$	$\Delta = 0.3$	$\Delta = 0.2$
Obtained Δ (Ours)	0.419	0.317	0.257	0.217
	$\beta = 10^3$	$\beta = 10^4$	$\beta = 10^5$	$\Delta_z = 0.5$
Obtained Δ (ERM)	1.0	1.0	1.0	-
Obtained Δ (CCC)	-	-	-	1.0

Table 1 shows that the proposed method outperforms both the baseline methods for the cartpole with softwalls system. The controller based on the ERM method in [18] achieves 100% constraint violation with $\beta = 10^4, 10^5$. With $\beta = 10^3$, the ERM results are comparatively better. One should
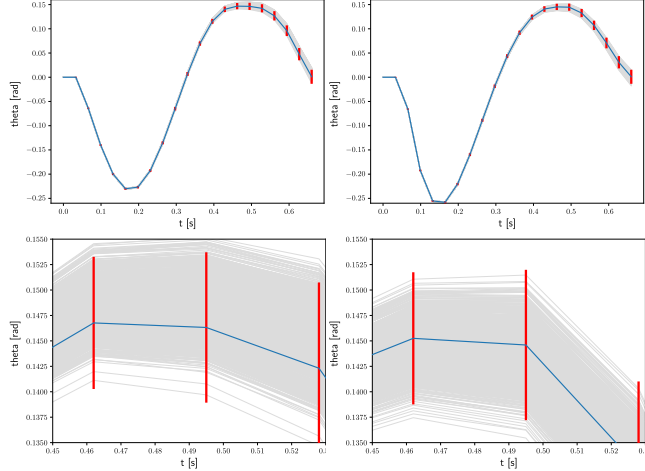
Figure 7: Simulated trajectories of x_2 of the cartpole example over 1000 samples with $\Delta = 0.5$ for the left column and with $\Delta = 0.02$ for the right column. The bottom row enlarges the top row figures around the area where the chance constraints effect is observed. The red line shows the 99.9 % confidence interval.

notice that higher weight of the ERM in the objective function results in more fragile trajectories since the state constraints are always violated. This indicates that the ERM-based objective is not able to capture the robustness in the state trajectories of SDLCS. The CCC in [19] could also show relatively good violation probability compared to the ERM-based method with $\beta = 10^4$ and $\beta = 10^5$ but shows the worse violation probability compared to our method with $\Delta = 0.5$ and the ERM with $\beta = 10^3$.

Table 2 shows similar results for the sliding box system for the proposed method. However, we observe that the controller can not satisfy the constraints for the cases with $\Delta = 0.01, 0.002$. There could be several reasons that contribute to the violation of the chance constraints. Unlike the cartpole example, F is not a P matrix for the sliding box system (see Section 5.2) so we can get the multiple solutions for the complementarity variable λ. Also, even though ϵ is small, it is not zero so the actual trajectory in the simulator cannot be exactly the same as the trajectory from the optimization even in the absence of noise. While we can ignore these effects with relatively large Δ, we cannot ignore these effects anymore with the small Δ. We believe some of these effects lead to some constraint violation observed for this system. Although the proposed method could not satisfy chance constraints for all Δ in this example, our method achieves much lower violation probabilities compared to the ERM in [18] and the CCC in [19]. Table 3 shows that we obtain similar results for the dual manipulator system as for the sliding-box example.

Fig. 7 and Fig. 8 show that our proposed planner could successfully drive the system to the goal state. We also observe that with decreasing Δ, the system trajectories move further away from state set boundaries to satisfy tighter chance constraints. For Fig. 9, while the majority of the sampled trajectories converge to the specified terminal constraints, some of them clearly converged to other states. This result also shows that the true distribution of the uncertainty for the SDLCS is not Gaussian.

5.5 Computation Results

We show computational time for the proposed method in Table 4. We observe that the compute time for our method increases as the number of integer variables increase. This is expected since we use mixed-integer programming. We also added the computational results for the ERM-based and
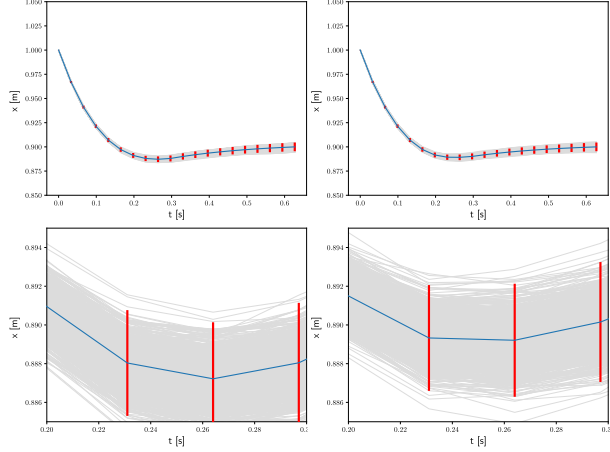
17

Figure 8: Simulated trajectories of x of sliding box with friction example over 1000 samples with $\Delta = 0.5$ for the left column and with $\Delta = 0.002$ for the right column. The bottom row enlarges the top row figures around the area where the chance constraints effect is observed. The red line shows the 99 % confidence interval.
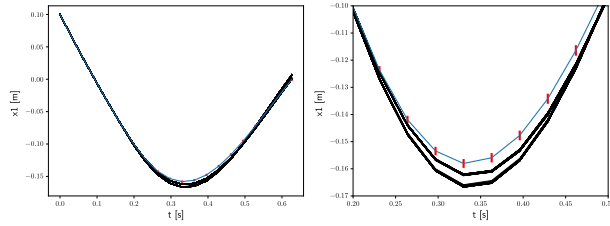

Figure 9: Simulated trajectories of x_1 over 1000 samples with $\Delta = 0.2$ for dual manipulation. The right figure shows the enlarged figure of the left figure. The red line shows the 99 % confidence interval.

the CCC method in Table 5. Similar to our method, both the ERM-based method and the CCC method incur larger computation time as the number of constraints and variables increase.

5.6   Discussion of Assumptions

In this section, we will provide empirical justification for the assumptions described in Section 3 that we made on the stochasticity of the matrices C, F and the determinism of the complementarity variable λ_{k+1}. Consider the cartpole system. Figure 10 plots simulated trajectories of the cartpole system for different realizations of the uncertain parameters. In performing the simulations, we simply sample the uncertainty in the spring constants and forward simulate the DLCS using the computed optimal controls obtained from our proposed optimization in (15). The subplots in 10a-10b plot the pole angle x_2 and the reaction force λ_2 for low value of uncertainty variance of 10^{-6} in the spring constants. The remaining plots 10c-10d and 10e-10f plot the same trajectories for larger uncertainty variances of 10^{-4} and $5 \cdot 10^{-4}$ respectively. In this specific scenario, x_1 and λ_1 trajectories are not shown since they do not show significant variation in the simulations. From these plots, we can observe that the simulated state trajectories x_2 (as light grey lines for sampling of uncertainty) are largely concentrated around the optimal trajectory of x_2 (blue line) computed from our proposed optimization approach (15). The main objective of the chance constraints is to control the state trajectories within prescribed limits. Our assumptions yield controls that precisely control the states as desired. The contact forces λ_2, in contrast to our assumption, are not

18

Table 4: Computation time of our method. $n_C, n_I, n_{\text{constraints}}$ show the number of continuous variables, the number of integer variables, and the number of total constraints, respectively, for each problem.

	n_C	n_I	$n_{\text{constraints}}$	runtime [s]
Cartpole with softwalls (Ours)	348	80	512	0.023
Sliding box (Ours)	220	120	624	1.95
Dual manipulation (Ours)	720	300	1632	8.29
Planar pushing (Ours)	148	40	270	0.009

Table 5: Computation time of other methods. $n_{\text{variables}}$ and $n_{\text{constraints}}$ show the total number of variables and the number of total constraints, respectively, for each problem.

	$n_{\text{variables}}$	$n_{\text{constraints}}$	runtime [s]
Cartpole with softwalls (ERM)	416	400	0.319
Cartpole with softwalls (CCC)	1178	1160	2.42
Sliding box (ERM)	437	420	0.281
Sliding box (CCC)	1328	1310	2.90
Dual manipulation (ERM)	737	720	0.701
Dual manipulation (CCC)	1468	1450	8.01

necessarily deterministic. However, our approach is able to capture the uncertainty propagation in the states and effectively contain the variance as desired. We have observed a similar behavior in the other systems considered in this paper. We believe a more rigorous theoretical justification can be provided and we will investigate this in a future work.

6 SMPC for Planar Pushing

In this section, we verify our proposed SMPC algorithm for contact-rich system can track a reference trajectory with probabilistic guarantees and outperform a deterministic MPC method. We demonstrate the proposed method for a stochastic pusher-slider system.

6.1 Planar Pushing

The frictional interaction between the pusher and slider leads to a linear complementarity system which we describe next. The pusher interacts with the slider by exerting forces in the normal and tangential directions denoted by $f_{\overrightarrow{n}}$, $f_{\overrightarrow{t}}$ (as shown in Figure 11) as well as a torque τ about the center of the mass of the object. Assuming quasi-static interaction, the limit surface [40] defines an invertible relationship between applied wrench $\mathbf{w}$ and the twist of the slider $\mathbf{t}$. The applied wrench $\mathbf{w}$ causes the object to move in a perpendicular direction to the limit surface $\mathbf{H}(\mathbf{w})$. Consequently, the object twist in body frame is given by $\mathbf{t} = \nabla \mathbf{H}(\mathbf{w})$, where the applied wrench $\mathbf{w} = [f_{\overrightarrow{n}}, f_{\overrightarrow{t}}, \tau]$ could be written as $\mathbf{w} = \mathbf{J}^T(\overrightarrow{n} f_{\overrightarrow{n}} + \overrightarrow{t} f_{\overrightarrow{t}})$. For the contact configuration shown in Figure 11, the normal and tangential unit vectors are given by $\overrightarrow{n} = [1 \quad 0]^T$ and $\overrightarrow{t} = [0 \quad 1]^T$. The Jacobian $\mathbf{J}$ is given by $\mathbf{J} = \begin{bmatrix} 1 & 0 & -p_y \\ 0 & 1 & p_x \end{bmatrix}$.

The dynamics of the pusher-slider system is given by

$$\dot{\mathbf{x}} = \mathbf{f}(\mathbf{x}, \mathbf{u}) = \begin{bmatrix} \mathbf{Rt} & \dot{p}_y \end{bmatrix}^\top \tag{21}$$
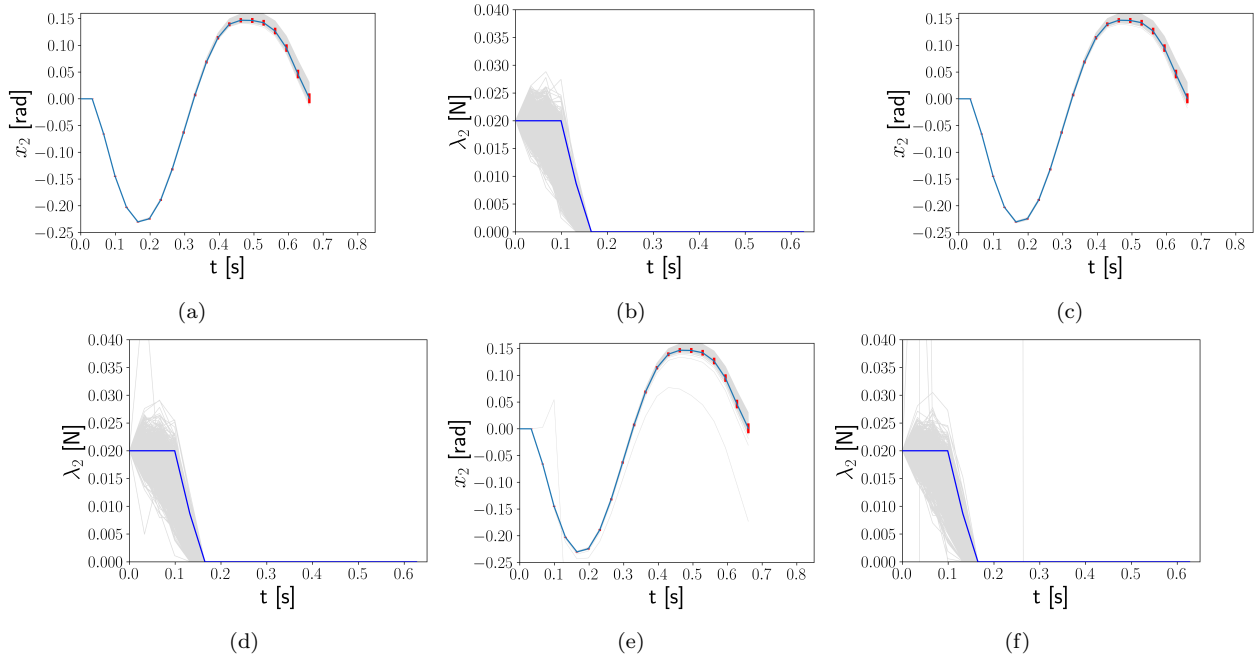
Figure 10: Trajectories for the stochastic cartpole system obtained by using 1000 samples for the uncertain parameters while the control input is set to that computed using our proposed optimization (15) where the uncertainty values correspond to those used in Section 5.2.1. (a): simulated trajectories of x_2 with uncertain $\frac{1}{k_1}, \frac{1}{k_2}$ for which standard deviations are 10^{-6}. (b): the simulated force trajectories of λ_2 corresponding to (a). (c): simulated trajectories of x_2 with uncertain $\frac{1}{k_1}, \frac{1}{k_2}$ which standard deviations are 10^{-4}. (d): the simulated force trajectories of λ_2 corresponding to (c). (e): simulated trajectories of x_2 with uncertain $\frac{1}{k_1}, \frac{1}{k_2}$ which standard deviations are $5 * 10^{-4}$. (f): the simulated force trajectories of λ_2 corresponding to (e). We rollout dynamics with the control input u which was computed (15), the blue lines show the optimal x_2, λ_2 and the rollouts are shown in grey.
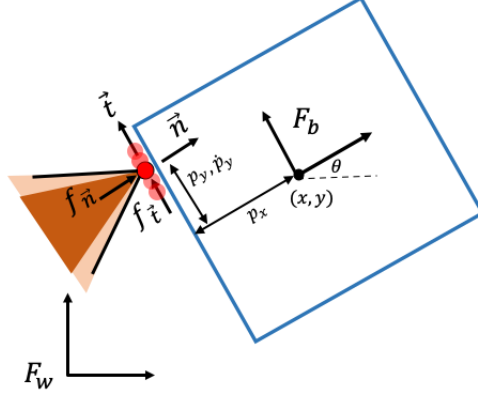
Figure 11: A schematic of a planar pusher-slider system. State of the system is $[x, y, \theta, p_y]^\top$ assuming that the pusher only comes in contact with the left edge as shown in the figure.

where $\mathbf{R}$ is the rotation matrix. The twist $\mathbf{t}$ can be obtained using an approximate limit surface [40] for quasi-static pushing. Since the wrench applied on the system depends of the point of contact of pusher and slider, the state of the system is given by $\mathbf{x} = [x \quad y \quad \theta \quad p_y]^\top$ and the input is given by $\mathbf{u} = [f_{\vec{n}} \quad f_{\vec{t}} \quad \dot{p}_y]^\top$. The elements of the input vector must follow the laws of coulomb friction which can be expressed as complementarity conditions as follows:

$$
\begin{aligned}
0 \le \dot{p}_{y+} \perp \mu_p f_{\vec{n}} - f_{\vec{t}} \ge 0 \\
0 \le \dot{p}_{y-} \perp \mu_p f_{\vec{n}} + f_{\vec{t}} \ge 0
\end{aligned}
\tag{22}
$$

where $\dot{p}_y = \dot{p}_{y+} - \dot{p}_{y-}$ and the μ_p is the coefficient of friction between the pusher and the slider.

The world frame and the body frame of reference are denoted by F_w and F_b respectively. The uncertainty in the friction cone is approximately represented by the shaded region in the friction cone. We use a modified version of (17) to solve SMPC for planar pusher-slider system. We use $0 \le u_{k,i}^e + u_{k,i}^* \le M z_{k,i,0}$ instead of (17e) because we have stochastic complementarity constraints on u, not on λ. We use the following hyper parameters: $\mu = 0.3, m = 1.0$. We use $dt = 0.1$ to discretize the dynamics and set $N = 10, M = 20$. We add uncertainty in μ and dynamics for which the standard deviations are 10^{-4} and 4×10^{-3}, respectively. We consider the following chance constraints: $\Pr(x^* - 0.1 \le x_{1,k} \le x^* + 0.1) \ge 1 - \frac{\Delta}{4N}$, $\Pr(x_{2,k} \le 0.27) \ge 1 - \frac{\Delta}{4N}$. The initial and the terminal state are $x_s = [0, 0, 0]^\top$, $x_g = [0, 0.2, \pi]^\top$. Also, we formulate our Deterministic MPC (DMPC) which uses the constraints $x_k \in \mathcal{X}$ instead of $\Pr(x_k \in \mathcal{X})$. We also evaluate the no-mpc case which implements the reference control sequence in open-loop.

6.2 Results

We evaluate the performance of the controllers with respect to:

(i) the safety in terms of the chance constraints by counting the number of failures, and

(ii) the Mean Squared tracking Error (MSE) from the reference trajectory.

Note that a failure is defined as constraint violation. Similar to the previous section, we use Monte Carlo simulations to evaluate the different controllers.

The obtained Δ and the MSE are shown in Table 6. Our proposed SMPC achieves the best performance with respect to both metrics followed by DMPC method. Since our proposed SMPC
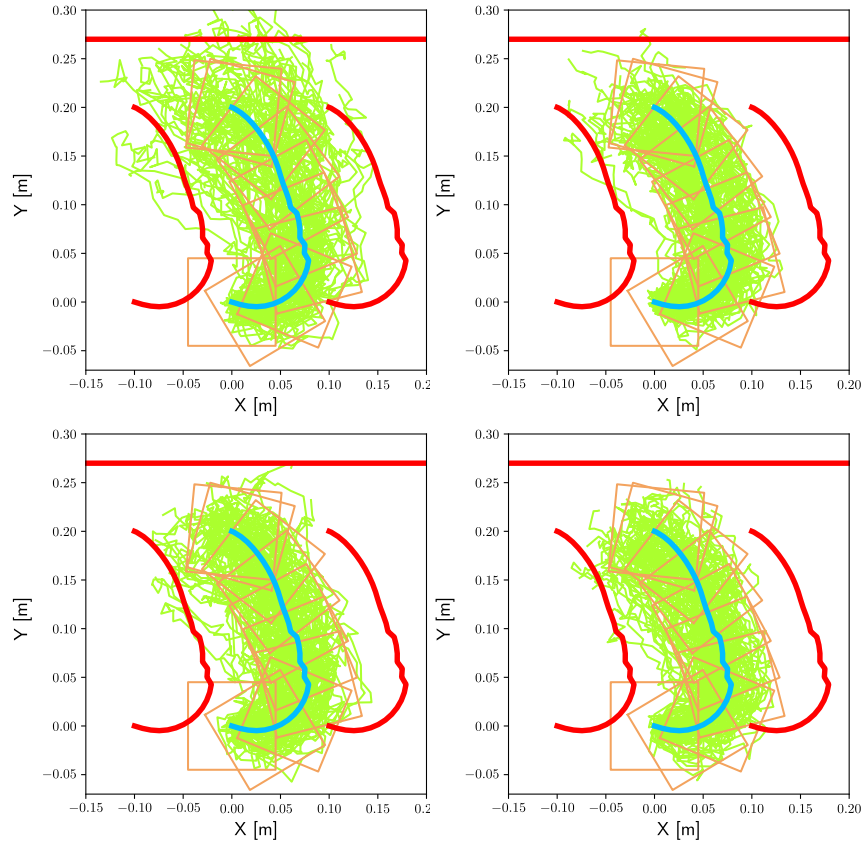
Figure 12: This figure shows results for the proposed SNMPC and comparison against some baseline approaches. Top left: no mpc (open loop), top right: DMPC, bottom left: $\Delta = 0.5$, bottom right: $\Delta = 0.01$. The blue curve shows the reference trajectory of the center of the box and the green lines show the simulated trajectories. The red curves show the bounds. As could be observed from the plots, we observe maximum constraint violation for the open-loop and deterministic MPC cases. Our proposed method with $\Delta = 0.01$ achieves best constraint satisfaction.

Table 6: Comparison of obtained Δ and MSE with different Δ from the simulation of "pushing with slipping" over 100 samples.

	No MPC	DMPC	$\Delta = 0.5$	$\Delta = 0.01$
Obtained Δ	0.31	0.19	0.10	0.00
MSE	0.00295	0.00244	0.00208	0.00216

considers stochastic complementarity constraints as well as uncertainty propagation, our method achieves lowest tracking error as well as constraint violation probability. We can see the trade-off between $\Delta = 0.5$ and $\Delta = 0.01$ where $\Delta = 0.5$ shows the higher Δ but the lower MSE. The reason why the DMPC shows higher MSE is that the DMPC may diverge from the reference trajectory since it ignores uncertainty propagation.

Fig. 12 illustrates the trajectories of MPC with different parameters. We can confirm that our proposed SMPC can track the reference trajectories while satisfying the chance constraints. Also, the average runtime for our SMPC to compute a solution was 0.0029 s during runtime.

7   Discussion and Conclusion

The hybrid dynamics of contact-rich interaction as well as uncertainty associated with contact parameters make efficient design of model-based controllers for manipulation challenging. We believe that understanding stochastic and robust optimization and control methods for contact-rich systems is important. However, this topic remains relatively unexplored in literature. One of the key reasons is the difficulty in handling stochastic complementarity constraints and its effect on uncertainty propagation for planning. This poses unique challenges for formulation of computationally feasible algorithms for robust planning of SDLCS.

In this paper, we presented a robust trajectory optimization technique for contact-rich systems. We presented a formulation for chance constrained optimization for SDLCS which is solved using MIQPCC. This paper makes an assumption of deterministic complementarity variables for computational tractability. We show that despite this assumption, we are able to compute controllers that are robust to the underlying stochastic system. We compared our proposed approach against other recent techniques for robust optimization for stochastic complementarity systems. We showed that our formulation outperforms these baseline techniques. We show that the proposed chance constrained optimization can be used to design stochastic MPC controllers for contact-rich system. The proposed SMPC was demonstrated for a stochastic planar pushing system.

In the future, we would like to relax certain assumptions in this work. We would like to propose solutions for general non-linear stochastic complementarity systems in the presence of non-Gaussian noise. In the current work, using joint chance constraints on all the variables results in conservative solutions. To consider these problems, the study of nonlinear uncertainty propagation in SNCS is required. Further, extending the approach to SNCS will result in the formulation falling in the class mixed-integer non-linear programming which can be difficult to solve. We would also like to investigate how we can relax the conservative solutions obtained by our proposed approach using better measures for risk. We would also like to incorporate real-time sensor input [41] to develop algorithms for stochastic model predictive control of complex manipulation problems [25, 11, 12].

References

[1] B. Brogliato, Nonsmooth mechanics, Vol. 3, Springer, 1999.

[2] E. Todorov, Implicit nonlinear complementarity: A new approach to contact dynamics, in: Proc. 2010 IEEE Int. Conf. Robot. Automat., IEEE, 2010, pp. 2322–2329.

[3] E. Drumwright, D. A. Shell, An evaluation of methods for modeling contact in multibody simulation, in: Proc. 2011 IEEE Int. Conf. Robot. Automat., IEEE, 2011, pp. 1695–1701.

[4] E. Drumwright, D. Shell, Modeling contact friction and joint friction in dynamic robotic simulation using the principle of maximum dissipation, in: Algorithmic foundations of robotics IX, Springer, 2010, pp. 249–266.

[5] M. Anitescu, F. A. Potra, Formulating dynamic multi-rigid-body contact problems with friction as solvable linear complementarity problems, Nonlinear Dynamics 14 (3) (1997) 231–247.

[6] Y. Shirai, X. Lin, Y. Tanaka, A. Mehta, D. Hong, Risk-aware motion planning for a limbed robot with stochastic gripping forces using nonlinear programming, IEEE Robot. Autom. Lett. 5 (4) (2020) 4994–5001. doi:10.1109/LRA.2020.3001503.

[7] S. C. Billups, K. G. Murty, Complementarity problems, Journal of Computational and Applied Mathematics 124 (1) (2000) 303–318, numerical Analysis 2000. Vol. IV: Optimization and Nonlinear Equations. doi:https://doi.org/10.1016/S0377-0427(00)00432-5.
URL https://www.sciencedirect.com/science/article/pii/S0377042700004325

[8] W. Heemels, J. M. Schumacher, S. Weiland, Linear complementarity systems, SIAM journal on applied mathematics 60 (4) (2000) 1234–1269.

[9] A. U. Raghunathan, D. K. Jha, D. Romeres, PYROBOCOP : Python-based robotic control & optimization package for manipulation and collision avoidance, CoRR abs/2106.03220 (2021). arXiv:2106.03220.

[10] S. Jin, D. Romeres, A. Ragunathan, D. K. Jha, M. Tomizuka, Trajectory optimization for manipulation of deformable objects: Assembly of belt drive units, arXiv preprint arXiv:2106.00898 (2021).

[11] Y. Shirai, D. K. Jha, A. U. Raghunathan, Robust pivoting manipulation using contact implicit bilevel optimization, arXiv preprint arXiv:2303.08965 (2023).

[12] Y. Shirai, D. K. Jha, A. U. Raghunathan, D. Hong, Tactile tool manipulation, arXiv preprint arXiv:2301.06698 (2023).

[13] M. Posa, C. Cantu, R. Tedrake, A direct method for trajectory optimization of rigid bodies through contact, Int. J. Rob. Res. 33 (1) (2014) 69–81.

[14] M. K. Camlibel, J.-S. Pang, J. Shen, Lyapunov stability of complementarity and extended systems, SIAM J Optimization 17 (4) (2006) 1056–1101.

[15] A. Aydinoglu, P. Sieg, V. M. Preciado, M. Posa, Stabilization of complementarity systems via contact-aware controllers, IEEE Transactions on Robotics 38 (3) (2021) 1735–1754.

[16] A. U. Raghunathan, J. L. Linderoth, Stability analysis of discrete-time linear complementarity systems, arXiv (2020).
URL `arXiv:2012.13287`

[17] X. Chen, M. Fukushima, Expected residual minimization method for stochastic linear complementarity problems, Mathematics of Operations Research 30 (4) (2005) 1022–1038.

[18] L. Drnach, Y. Zhao, Robust trajectory optimization over uncertain terrain with stochastic complementarity, IEEE Robot. Autom. Lett. 6 (2) (2021) 1168–1175.

[19] L. Drnach, J. Z. Zhang, Y. Zhao, Mediating between contact feasibility and robustness of trajectory optimization through chance complementarity constraints, Front. Robo. AI 8 (2021).

[20] A. Ben-Tal, L. El Ghaoui, A. Nemirovski, Robust optimization, Princeton university press, 2009.

[21] Y. Tassa, E. Todorov, Stochastic complementarity for local control of discontinuous dynamics, in: Proceedings of Robotics: Science and Systems, Zaragoza, Spain, 2010. doi:10.15607/RSS.2010.VI.022.

[22] Y. Shirai, D. K. Jha, A. Raghunathan, D. Romeres, Chance-constrained optimization in contact-rich systems for robust manipulation, arXiv preprint arXiv:2203.02616 (2022).

[23] Z. Manchester, S. Kuindersma, Variational contact-implicit trajectory optimization, in: Robotics Research, Springer, 2020, pp. 985–1000.

[24] S. L. Cleac'h, T. Howell, M. Schwager, Z. Manchester, Fast contact-implicit model-predictive control, arXiv preprint arXiv:2107.05616 (2021).

[25] Y. Shirai, D. Jha, A. Raghunathan, D. Romeres, Robust pivoting: Exploiting frictional stability using bilevel optimization, in: Proc. 2022 IEEE Int. Conf. Robot. Automat., 2022, p. accepted.

[26] A. Prékopa, Boole-bonferroni inequalities and linear programming, Operations Research 36 (1) (1988) 145–162. doi:10.1287/opre.36.1.145.

[27] Y. Shirai, D. K. Jha, A. U. Raghunathan, Covariance steering for uncertain contact-rich systems (2023). arXiv:2303.13382.

[28] L. Blackmore, M. Ono, B. C. Williams, Chance-constrained optimal path planning with obstacles, IEEE Transactions on Robotics 27 (6) (2011) 1080–1094. doi:10.1109/TRO.2011.2161160.

[29] K. Okamoto, P. Tsiotras, Optimal stochastic vehicle path planning using covariance steering, IEEE Robot. Autom. Lett. 4 (3) (2019) 2276–2281. doi:10.1109/LRA.2019.2901546.

[30] A. Wang, A. Jasour, B. C. Williams, Non-gaussian chance-constrained trajectory planning for autonomous vehicles under agent uncertainty, IEEE Robot. Autom. Lett. 5 (4) (2020) 6041–6048. doi:10.1109/LRA.2020.3010755.

[31] R. Cottle, J. Pang, R. Stone, The Linear Complementarity Problem, Classics in Applied Mathematics, Society for Industrial and Applied Mathematics, 2009.

[32] M. Zhang, D. K. Jha, A. U. Raghunathan, K. Hauser, Simultaneous trajectory optimization and contact selection for multi-modal manipulation planning, arXiv preprint arXiv:2306.06465 (2023).

[33] A. Schperberg, S. Tsuei, S. Soatto, D. Hong, Saber: Data-driven motion planner for autonomously navigating heterogeneous robots, IEEE Robot. Autom. Lett. 6 (4) (2021) 8086–8093. doi:10.1109/LRA.2021.3103054.

[34] O. Celik, H. Abdulsamad, J. Peters, Chance-constrained trajectory optimization for non-linear systems with unknown stochastic dynamics, in: 2019 IEEE/RSJ International Conference on Intelligent Robots and Systems (IROS), 2019, pp. 6828–6833. doi:10.1109/IROS40897.2019.8967794.

[35] J. Z. Zhang, L. Drnach, Y. Zhao, Mediating between contact feasibility and robustness of trajectory optimization through chance complementarity constraints, CoRR abs/2105.09973 (2021). arXiv:2105.09973.

[36] F. R. Hogan, A. Rodriguez, Reactive planar non-prehensile manipulation with hybrid model predictive control, Int. J. Rob. Res. 39 (7) (2020) 755–773. doi:10.1177/0278364920913938.

[37] Gurobi Optimization, LLC, Gurobi Optimizer Reference Manual (2021).
URL https://www.gurobi.com

[38] A. U. Raghunathan, D. K. Jha, D. Romeres, Pyrobocop: Python-based robotic control & optimization package for manipulation, in: 2022 International Conference on Robotics and Automation (ICRA), 2022, pp. 985–991. doi:10.1109/ICRA46639.2022.9812069.

[39] J. J. Moré, B. S. Garbow, K. E. Hillstrom, User guide for minpack-1, Tech. rep., CM-P00068642 (1980).

[40] S. Goyal, A. Ruina, J. Papadopoulos, Planar sliding with dry friction part 1. limit surface and moment function, Wear 143 (2) (1991) 307–330.

[41] S. Dong, D. Jha, D. Romeres, S. Kim, D. Nikovski, A. Rodriguez, Tactile-RL for insertion: Generalization to objects of unknown geometry, in: 2021 IEEE International Conference on Robotics and Automation (ICRA), 2021.